BZ-97: A Promising Compound Against *Trypanosoma cruzi*

Milixza M Botacio[1,2,] *, Maria F. Alves-Rosa[1,]*, Nerea Escala[3], Michele Ng[1], Lorena M. Coronado[1], Jafeth Carrasco[1], Doriana Dorta[1], Laura Pineda[1,] Esther del Olmo[3], Ricardo Correa[1, †], Carmenza Spadafora[1, †]

[1]Center of Cellular and Molecular Biology of Diseases, Instituto de Investigaciones Científicas y Servicios de Alta Tecnología (INDICASAT AIP), City of Knowledge, Clayton, Apartado 0816-02852, Panama City, Panama.
[2]Programa de Maestría en Microbiología Ambiental, Universidad de Panamá, Panama City, Rep. of Panama.
[3]Departamento de Ciencias Farmacéuticas: Química Farmacéutica, Facultad de Farmacia, Universidad de Salamanca, CIETUS, IBSAL, 37007, Salamanca, Spain.
†Corresponding authors' email: rcorrea@indicasat.org.pa,

Abstract

Chagas Disease has been considered "the most neglected among the neglected diseases." Only two very toxic drugs developed in the 1960s have been approved to control the disease in its acute phase and are infective in the chronic stage of the illness. It is imperative to find new molecules that can act against the causative parasite, *Trypanosoma cruzi.* BZ-97 is a synthetic product derived from the benzimidazole scaffold. It was tested against other human parasites, showing the best activity (IC50 = 0.76 µM) towards *T. cruzi* intracellular stages. The effects of BZ-97 on epimastigotes of the Y strain were analyzed. Signs of changes in the parasite homeostasis were evident by acidocalcisomes alkalinization, calcium mobilization, changes in their morphology and some signs of apoptotic events with a lack of ROS production, which is a crucial advantage over the behavior of the reference drug, benznidazole. Acidocalcisomes alkalinization was evidenced through fluorescence microscopy analysis and the use of 5-[N-ethyl-N-isopropyl] amiloride (EIPA), an inhibitor of the TcNHE pump, confirmed the involvement of this proton pump in the BZ-97-mediated acidocalcisome alkalinization. BZ-97 is presented as a potential lead compound against *T. cruzi that is* worthy of further studies in the future.

Keywords: *Trypanosoma cruzi*, anti trypanosomatid, acidocalcisome, benzimidazole scaffold

Introduction

*Trypanosoma cruz*i is the causative parasite of American Trypanosomiasis, better known as Chagas Disease. This ailment affects approximately 7-8 million people in Latin America (1). An annual incidence of 30,000 new cases and 10,000 deaths has been reported (2). However, as it is a silent disease, the number of infected people and deaths associated with this disease is probably imprecise and underestimated (3, 4). As a consequence of large waves of migration, a large percentage of people carry the infection to non-endemic areas such as North America (5).

CD has two phases: an initial acute phase, which is usually asymptomatic, and a lifelong chronic phase, which in 60 to 70% of patients is clinically silent, but 20 to 30% of them will develop in years or decades heart problems (20 to 30%), digestive problems, or a combination of both (10 to 15%). Neurological symptoms

---

* Both authors Milixza M Botacio and Maria F. Alves-Rosa contributed equally to the work.

are also seen in a small proportion of patients (5%) (6).

To kill the parasite, CD can be treated with Benznidazole (BNZ) or Nifurtimox (NFX), both developed over 40 years ago. Both compounds are currently the only drugs available for treating CD and remain as therapeutic options showing certain efficacy in the treatment of CD (7). While both, NFX and BNZ, are effective in treating the acute stages of infection, their efficacy is limited in the chronic phase and varies by geographical location (3).

Furthermore, the frequency of drug side effects is higher in older patients, further limiting their benefits. The treatment regimen with both compounds is long, and many adverse effects can occur, compromising the continuity of the treatment. Regarding the common adverse effects of BNZ, they include allergic dermatitis, nausea, vomiting, anorexia, weight loss, insomnia, and dose-dependent peripheral sensitive neuropathy, among others (8-10). Rare but serious events include neuropathy and bone marrow depression.

In the absence of effective and less toxic chemotherapies against Chagas Disease, new, safer, and more efficient drugs are urgently needed against this disease.

Nitroimidazoles are a well-known class of active compounds that have shown high activity against *T. cruzi* (11). The incorporation of a nitro group into the imidazole ring has been widely studied, as in Benznidazole (*N*-benzyl-2-(2-nitroimidazol-1-il)acetamide); on the other hand Benzimidazoles (BZ), that is, organic compounds that have a benzene ring linked to an imidazole ring in positions 4 and 5 have shown very interesting biological activities. BZ rings are considered good scaffolds for the development of new promising candidates against Chagas disease.

The structure of BZ is related to that of imidazole; however, taking into account their physicochemical properties, the former are weaker bases than the latter due to the benzene ring that can help delocalize electrons from the imidazole nitrogen through a variety of resonance conformations. BZ derivatives as the 2-aminoBZ type represent a group of compounds with interesting biological activity (12), and some of them are drugs of clinical uses as antifungal or anthelmintic properties (e.g. albendazole) among others (Figure 1).

Figure 1. Structures of Benzimidazole (left), Albenzadole (center), and Benznidazole (right)
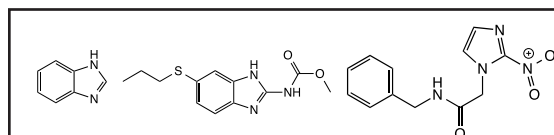
In lieu of the above, a number of new derivatives of BZ were synthesized and screened against tropical human parasites, including *Trypanosoma cruzi*. This report details the screening and characterization of the biological activity of one such derivative, BZ-97, against *T. cruzi*, the causative agent of Chagas Disease.

Materials and Methods

Chemical compounds

Compound BZ-97 was used in a previous study describing their synthesis (13). The derivative was kept as a lyophilized product that, when ready to be used, was prepared in stock solutions (5 mM) in 100% dimethyl sulfoxide (DMSO; Sigma-Aldrich®). It was stored at 4 ºC until the day of the experiment when it was taken to the corresponding concentration in the plate by diluting it in culture media (13). In the study presented here, compound BZ-1 was tested against Trypanosoma cruzi parasites with the code BZ-97.
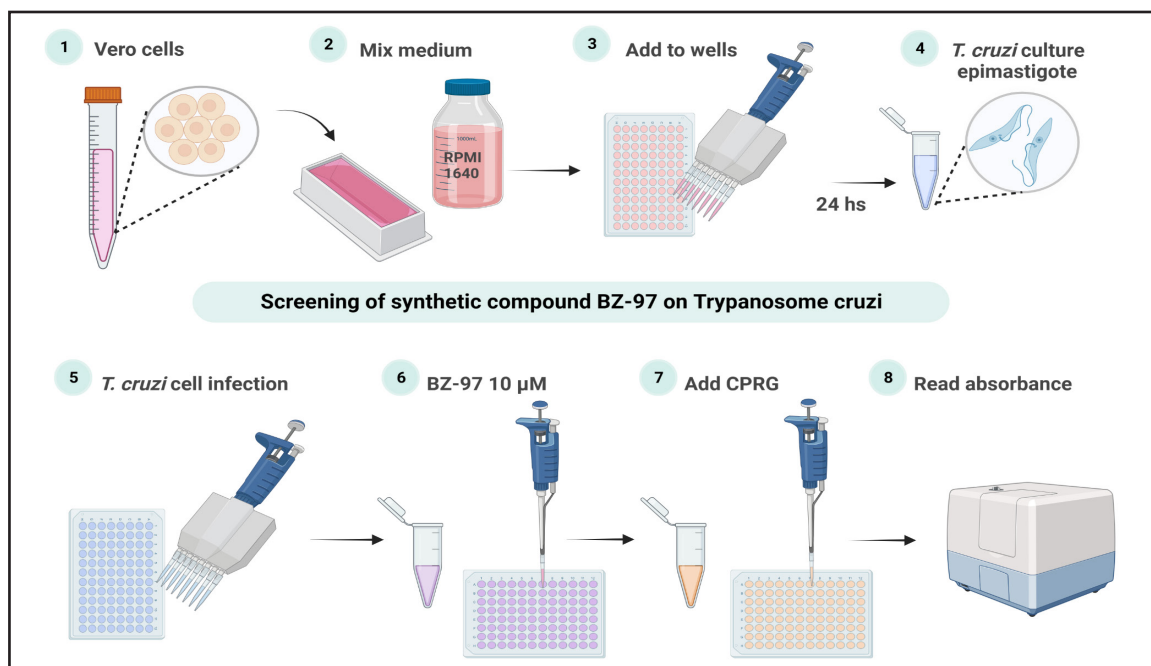
Parasites and bioactivity assays

Intracellular antitrypanosomal bioassays were carried out on the recombinant Tulahuen clone C4 lacZ of *T. cruzi* trypomastigotes (American Type Culture Collection (ATCC), Manassas, VA, USA), which expresses the

β-galactosidase enzyme as a reporter of viability (14, 15). Vero cells (ATCC, Manassas, VA) were grown for 24 hours prior to performing the experiment. On the day of the experiment, cells were infected, and BZ-97 was dissolved in DMSO and added to the medium at a single dose of 10 µM for screening purposes (Fig. 2) or at 10, 2, 0.4, and 0.1 µM, for the determination of its IC50. Infected cells were incubated for five days and maintained in RPMI-1640 at 37 °C under a 5% CO_2 atmosphere with L-glutamine, 4-(2-Hydroxyethyl)-piperazine-1-ethanesulfonic acid buffer, $NaHCO_3$, 10% FBS and 1% penicillin/streptomycin as supplements. To determine the anti-trypanosomal activity, chlorophenol-red-β-D-galactopyranoside (Roche Applied Science) was used as the substrate of living parasites β-galactosidase, which was allowed to act for 4.5 h. Benznidazole was used as a positive control using 10, 1, and 0.1 µg/ml to determine its IC50. Absorbance was measured at 570 nm using a plate reader (Sinergy HT, BioTek Instruments Inc, Winooski, VT, USA).

For epimastigote assays, the Y strain of *T. cruzi,* grown in LIT medium, was used, as it was chosen as the reference strain for drug discovery programs against Chagas Disease (15,16). Parasites at 5×10^6 epimastigotes/mL were incubated at 28 °C in 96-well plates, adding the compound BZ-97 at the concentrations described for the trypomastigote assays. Benznidazole and untreated parasites were used as positive and negative controls, respectively. The antiparasitic activity was evaluated

Figure No.2 . Diagram of the screening protocol used for the analysis of active compounds against *T. cruzi* of the Tulahuen strain (clon C4 lacZ) or Y.

after 72 h of incubation using the MTT method.

Cytotoxicity determination

For cytotoxicity assays, Vero cells were cultivated in 96-well plates with RPMI-1640 medium (Sigma- Aldrich, USA) supplemented with 1% penicillin/streptomycin and 10% fetal bovine serum (FBS) (Gibco, Invitrogen, Carlsbad, CA, USA). Cells were allowed to adhere to the bot-

tom of the flask for 24 h before incubating them with the compound for five days. DMSO, the vehicle for BZ-97, was used as a negative control. To obtain the IC50 of the drugs, BZ-97 was assayed at the same concentrations used in the anti-trypanosomal assay, and benznidazole was analyzed with 7 concentrations ranging from 500 to 7.8 µg/ml (1,921 to 30 µM). After incubation, MTT (3-(4, 5-dimethyl-thiazol-2-yl)-2, 5-di-phe-nyl-tetra-zoliµM bromide) at 2.5 µg/ml was added to each well. Absorbance was determined 4 h later at 570 nm, using a color plate reader, as described earlier by Mosmann et al, 1983 (16) and modified for *T. cruzi* by Muelas-Serrano et al, 2000 (17).

All bioassays were performed in duplicates and some in triplicates. The IC50 of Adriamycin, calculated from using 1, 10, and 100 nM concentrations, was used as a positive control for cytotoxicity assays.

Detection of reactive oxygen species

Measurement of intracellular reactive oxygen species (ROS) was evaluated through ROS-dependent 5-(and-6)-chloromethyl-2′,7′-dichlorodihydrofluorescein diacetate (CM-H2DCFDA) (Molecular Probes®, Eugene OR, USA) oxidation. The amount of oxidized DCF indicates the level of intracellular ROS production. Briefly, 10x6 epimastigotes were cultured in a 96-well plate and incubated with LIT medium (control), (20 µM) BZ-97, or (40 µM) BNZ for 3h at 28°C h. After that, parasites were loaded with CM-H2DCFDA (10 µM) and incubated in the dark for 30 min at room temperature. Intracellular ROS production was detected in a fluorometer (Biotek Synergy HT). Excitation was performed at 495 nm, and fluorescence emission was detected at 530 nm. 200 µM Hydrogen peroxide (H_2O_2)-treated epimastigotes were used as a positive control. Untreated parasites were used as a negative control. Intracellular ROS production was measured with a fluorometer.

Mitochondrial membrane potential (ΔΨM) changes

Mitochondrial membrane potential (ΔΨM) changes were evaluated using 3,3′-dihexyloxacarbocyanine iodide (DiOC6), a lipophilic, permeable dye that emits green fluorescence and demonstrates selectivity towards the mitochondria of living cells when used at low concentrations (18). DiOC6 accumulates in the mitochondria proportionally to the ΔΨm values. The experiments were performed using $5x10^5$ epimastigotes cultured in a 96-well plate and incubated with LIT medium (control), 20 µM BZ-97, or 40 µM BNZ for 3h, 6h and 9 h at 28°C. After that, cells were stained with 10 nM DiOC6 and incubated in the dark for 20 min at 28°C h. After staining, the parasites were washed and suspended in 200 µl of phosphate-buffered saline (PBS) and analyzed immediately by flow cytometry. $5x10^5$ epimastigotes were treated with 50 µM CCCP, a compound known to disrupt mitochondrial membranes, acting as a positive control for depolarization of the mitochondrial membrane.

Fluorescent microscopy

All epimastigote images were acquired after a drop of living parasites was placed on a clean glass slide, covered with a coverslip, and sealed. Epimastigotes were visualized with the appropriate lasers with an Olympus FV3000 confocal microscope (Olympus Corporation, Osaka, Japan). A 100 X objective was used to obtain the images.

Alkalinization of acidocalcisomes detection using acridine orange (AO)

Changes in the pH of the acidocalcisomes of epimastigotes were monitored by AO staining, a weak base that accumulates in acidic compartments. Its nonionized form dominates in neutral to alkaline environments, emitting green fluorescence and easily diffusing across membranes. In acidic environments, its ionized form prevails, emitting orange fluorescence and being membrane-impermeable (19). Thus, AO accumulation in acidic compartments can be detected as a bright green fluorescence (530 nm) when excited by a 488 nm laser. Thus,

$5x10^5$ epimastigotes cultured in a 96-well plate and incubated with LIT medium (control), 20 µM BZ-97; 40 µM BNZ, 5 µM Mannitol, 20 µM BZ-97 plus 5 µM 5-[N-ethyl-N-isopropyl] amiloride (EIPA); 40 µM BNZ plus 5 µM EIPA, or 1 µM Mannitol plus 5 µM EIPA for 3h at 28°C in 96-well plates. Subsequently, parasites were stained with 5 µM AO, which served as a probe for alkalinization and was then analyzed by fluorometry using a BioTek Sinergy HT fluorometer using the Gen 5 software.

In another set of experiments, $1x10^5$ epimastigotes were cultured in a 96-well plate and incubated with LIT medium (control) or 20 µM BZ-97 for 24 h at 28°C. Parasites were stained with 5 µM OA for 20 minutes in the dark and washed twice with 200 µl of PBS. A 488 nm laser was used to excite the stain.

Alkalinization of acidocalcisomes detection using LysoSensor™

The LysoSensor™ dye is an acidotropic probe that accumulates in acidic organelles due to protonation. This pH-dependent process also causes the fluorescence quenching of the dye by its weak base side chain to be released, leading to higher fluorescence intensity. LysoSensor staining was performed according to the protocol described by Albrecht et al, 2020 (20), with minor modifications. Briefly, $5x10^5$ epimastigotes were incubated with LIT medium (control), 20 µM BZ-97, 40 µM BNZ, or 20 µM BZ-97 plus 5 µM EIPA for 24 h at 28°C in 96 well plates. After this period of time, the medium containing the stimulus was carefully removed, and 1 µM LysoSensor was added with a freshly tempered LIT medium and incubated for 30 min at 28°C. Subsequently, epimastigotes were washed 3 times with cold PBS (200 µl per wash), mounted on slides, and sealed with a coverslip. The cell-associated green fluorescence (excited with a 488 nm laser) was analyzed in a fluorescent microscope. A comparative analysis of fluorescence intensity was done with the ImageJ software (NIH, USA).

Fluorescence microscopy image processing

Fluorescence microscopy images were processed and analyzed through the Image processing free download software ImageJ 1.x developed by the National Institutes of Health and the Laboratory for Optical and Computational Instrumentation (LOCI, University of Wisconsin) (https://imagej.net/software/imagej).

The data were expressed as the fluorescence intensity value of compound-treated epimastigotes (FI) over baseline (control, LIT medium-treated epimastigotes).

Propidium iodide (PI) staining

Cell membrane damage in epimastigotes can be assayed by quantifying the level of PI incorporated inside treated cells. Briefly, $10x^6$ epimastigotes were cultured in a 96-well plate and incubated with LIT medium (control), 20 µM BZ-97 or 40 µM BNZ for 3 h at 28°C in 96-well plates. Cells were washed once with PBS, and parasites were then resuspended in PBS containing 1 µM PI. Untreated parasites were used as the negative control. As a positive control of cellular damage, epimastigotes were subjected to a high temperature 80 °C in a thermostatic bath for 30 min. Each sample's mean fluorescence intensity (MFI) was determined using the 535 nm laser of a ParteQ CyFlow cytometer (Germany). The experiment was repeated twice in quadruplicates.

Changes in cell viability through apoptosis or necrosis

Apoptosis/ necrosis cellular death was evaluated by flow cytometry using FITC-labeled Annexin V and red-fluorescent propidium iodide (PI) staining (Alexa Fluor™ 488 annexin V/Dead Cell Apoptosis Kit, from Invitrogen™). The assay was performed according to manufacturer instructions with minor modifications. Briefly, 5 x 10^5 epimastigotes were treated with LIT medium (control), 20 µM BZ-97, 40 µM BNZ, or 1 µM staurosporine for 6 and 24 h at 28°C in 96-well plates. Then, the cells were rinsed once with LIT medium, gently resuspended in 100 µL Annexin V reagent, and incubated in the dark for 15

minutes at 28°C h. The reaction was stopped by adding 200 µL of 1X binding buffer, and cells were analyzed by flow cytometry within one hour for maximum signal. The mean fluorescence intensity (MFI) of FL2 (PI) and FL1 (Annexin V) of each sample was determined using the 535 nm laser of a flow cytometer. All experiments were repeated at least twice in quadruplicates.

Statistical analysis

All experiments were repeated at least twice in quadruplicates. Flow cytometry data are representative of three independent experiments unless otherwise stated. Graphical and One-way ANOVA with Bonferroni's post hoc statistical analysis were performed using GraphPad Prism version 6.04 for Windows, GraphPad Software, (www.graphpad.com)

Results and Discussion

Anti-trypanosomal activity

During screening of possible antiparasitic compounds, BZ-97 performed well in the low micromolar levels against three parasites: *Leishmania donovani, Trypanosoma cruzi, and Plasmodium falciparum*. The best action was directed against *T. cruzi,* with sub micromolar values (Table I).

Table I. Effect of BZ-97 on intracellular human parasites

INTRACELLULAR BIOASSAYS				Selectivity Index for *T. cruzi*
BZ-97 IC50 (uM)				
L. donovani	*T. cruzi*	*P. falciparum*	Vero cells	
1.33	0.76	1.02	11.5	15.1

Given the results obtained in the BZ-97 intracellular IC50 assays, we decided to further study this molecule's effects against *T. cruzi.* A head-to-head anti-*T. cruzi* test was performed to evaluate the effect of this compound on the death of the epimastigotes, comparing it with benznidazole (BNZ), the reference compound.

Both BZ-97 and BNZ seem to be less potent against epimastigotes than they were against intracellular forms of the parasite (Table II)

Table II. IC50 of compounds on T. cruzi epimastigotes

BZ-97 IC50 (uM)			Selectivity Index
	T. cruzi epimastigotes	Vero cells	
BZ-97	2.03 ± 1.17	11.5 ± 1.8	5.1
Benznidazol	4.59 ± 0.70	47.1 ± 7.0	10.3

Effect of BZ-97 on reactive oxygen species production

It is known that ROS production is a marker of alterations in the parasite's homeostasis caused by various factors, including pH fluctuation, stress, hypoxia, and the presence of heme. The data depicted in Figure 3 show that epimastigotes treated with 20 µM BZ-97 for 3 h do not differ significantly in ROS production from non-treated cells. On the contrary, 40 µM BNZ-treated epimastigotes show an 8-fold increase in ROS synthesis compared with parasites not challenged with any external stimulus. The addition of 200 µM H_2O_2 serves the purpose of verifying the integrity of the reagents and analytics used in this experiment.
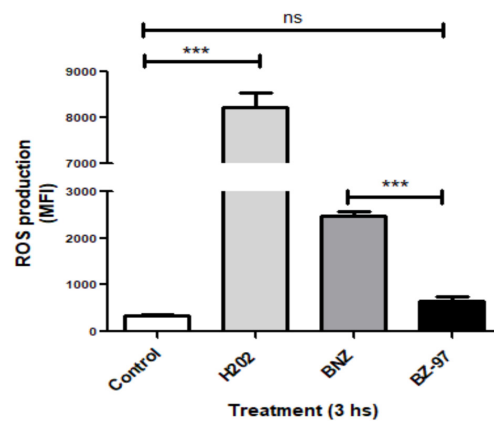

Figure 3. Effect of BZ-97 on epimastigote ROS production.

T. cruzi epimastigotes were cultured in

the presence of LIT medium (control), 20 µM BZ-97, 40 µM BNZ, or 200 µM H_2O_2 for 3 h prior to detection of ROS production by flow cytometry. Samples were measured with four replicates in each of three independent experiments. MFI: Mean Fluorescence Intensity. One-way ANOVA and Bonferroni's Multiple Comparison Test were used to measure significant variation compared to the untreated control at each time point; *** p <0.001; ns: not significant.

Effect of BZ-97 on mitochondrial transmembrane potential

Viable epimastigotes were treated with LIT medium (control), 20 µM BZ-97 or 40 µM BNZ for 3, 6 and 9 h and changes in the trans-

membrane potential were analyzed by flow cytometry. Results depicted in Figure 4 indicate that while BNZ induces a depolarization of the mitochondrial membrane, at 3 and 6 h, reflected by a decrease in the DiOC6 mean fluorescence intensity (MFI), BZ-97 does not exhibit significant changes at the same time points. The effect of BNZ is reversed at 9 h, showing no significant differences in the DiOC6 MFI compared to either BZ-97 or untreated cells. In these experiments, the low MFI exhibited by CCCP-treated epimastigotes, an inhibitor of mitochondrial oxidative phosphorylation, indicates complete and irreversible depolarization (CCCP-treated vs untreated epimastigotes MFI, *** p< 0.0001).

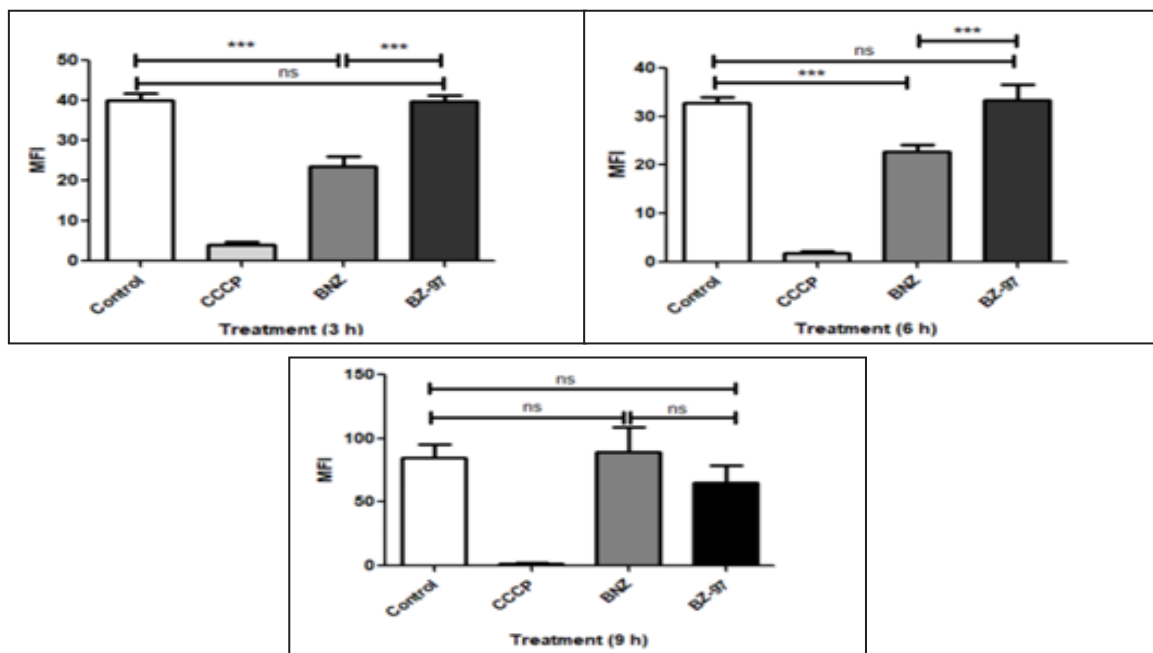

Figure 4. Effects of BZ-97 on the Mitochondrial Membrane Potential in T. cruzi epimastigotes.

Epimastigotes from *T. cruzi* strain Y were incubated with LIT medium (control), 20 µM BZ-97 or 40 µM BNZ for 3, 6 and 9 h before evaluating changes in mitochondrial membrane polarization by flow cytometry. 50 µM CCCP was used as the positive control. MFI: Mean Fluorescence Intensity. One-way ANOVA and Bonferroni's Multiple Comparison Test were used.

*** p <0.001; ns: no significant difference.

Effect of BZ-97 on the acidity of acidocalcisomes

To evaluate the effect of BZ-97 treatment on epimastigote acidocalcisomes, we further assessed changes in the acidity of this organelle caused by treatments for 3 h using

acridine orange (AO) staining. Fluctuations in the organelle's proton (H+) content are reflected by changes in the AO fluorescence at 530 nm emission.

Figure 5 shows that 20 µM BZ-97-treated epimastigotes exhibit a highly significant increase in AO absorbance, indicative of acidocalcisome alkalinization; similar results were observed in 40 µM BNZ-treated cells. In addition, both compounds show no significant differences in their AO absorbance levels.

EIPA abrogates the effect of BZ-97 and BNZ on acidocalcisomes, resulting in absorbance values similar to those of control cells. Additionally, 5 µM Mannitol strongly induces acidocalcisome alkalinization, and this effect is not prevented by EIPA.
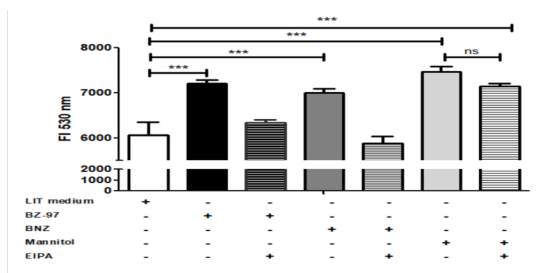

Figure 5. Effect of BZ-97 on acidocalcisomes of epimastigotes.

T. cruzi epimastigotes were treated with LIT medium (control), 20 µM BZ-97, 40 µM BNZ or 5 µM Mannitol (positive alkalinization control) with or without 5 µM EIPA for 3 h. 5 µM OA was added to all groups, and their fluorescence was analyzed by fluorometry. FI 530 nm = Fluorescence Intensity at 530 nm One-way ANOVA and Bonferroni's Multiple Comparison Test were used. *** $p < 0.001$; ns: no significant difference.

Fluorescence microscopy (FM) of acidocalcisomes of BZ-97-treated epimastigotes

To verify if the observed effect of BZ-97 on the alkalinization of acidocalcisomes persists over time, viable epimastigotes were grown at exponential phase and then treated with LIT medium (control), 20 µM BZ-97, 20 µM BZ-97 + 5 µM EIPA or 40 µM BNZ for 24 h.

Results obtained from FM using Lyso-Sensor™ as an acidic organelle detector probe are depicted in Figure 6. In control epimastigotes, these organelles are visualized as clearly defined green points with high fluorescence intensity (Fig 6A). In contrast, acidocalcisomes from BZ-97- treated epimastigotes show spots with blurry boundaries and lower fluorescence intensity, indicative of acidocalcisome alkalinization (Fig 6B).

BNZ treatment also induces changes in the fluorescence signal similar to BZ-97 (Fig 6C), while incubation of epimastigotes with BZ-97 and EIPA (an inhibitor of primarily Sodium-Hydrogen Exchangers (NHEs) abrogates the effect of BZ-97 (Fig 6D) showing well-defined high fluorescent intracellular spots.
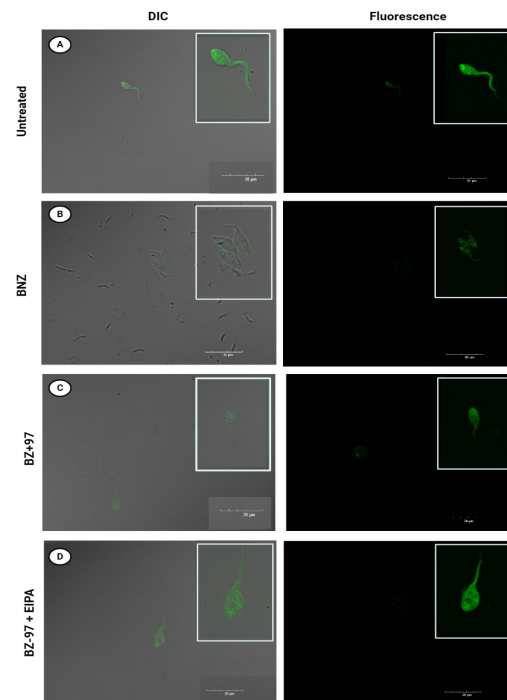

Figure 6. Fluorescence Microscopy of acidocalcisomes of BZ-97-treated epimastigotes using LysoSensor Green probe.

Changes in the pH of acidic organelles of live epimastigotes of *T. cruzi* were assayed using the LysoSensor Green probe. Untreated epimastigotes (A), epimastigotes treated with 20 µM BZ-97 (B), 20 µM BZ-97 + 5 µM EIPA (C), or 40 µM BNZ (D) incubated for 24 h are shown. Inset images have been subjected to digital processing to enhance visualization of parasites. Brightness, exposure, and contrast adjustments were applied solely to improve clarity of these specific regions. All insets received identical image correction parameters to maintain consistency. DIC: differential interference contrast. Pictures are representative of more than 15 fields of one experiment.

These results were also confirmed using acridine orange (AO)-stained epimastigotes. AO is a fluorescent dye that can selectively stain acidic organelles. Untreated epimastigotes exhibited discrete tiny spots throughout the parasite cytoplasm indicative of the presence of acidocalcisomes, and this feature is much less intense after BZ-97 treatment (Figure 7).
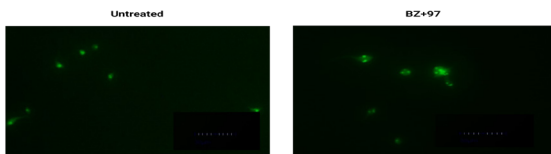

Figure 7. Fluorescence Microscopy (FM) of acidocalcisomes of BZ-97-treated epimastigotes using acridine orange (AO) staining**.**

Changes in the pH of acidic organelles of live epimastigotes of *T. cruzi* were assayed using acridine orange (AO). Untreated epimastigotes and epimastigotes treated with 20 µM BZ-97 for 24 h were subjected to 5 µM acridine orange (AO) staining. Pictures are representative of more than 15 fields of one experiment. Bar = 30 µm.

FM images were processed and analyzed through the Image processing software ImageJ 1.x Figure 8. Statistical analysis supports the conclusions driven from the FM assay.
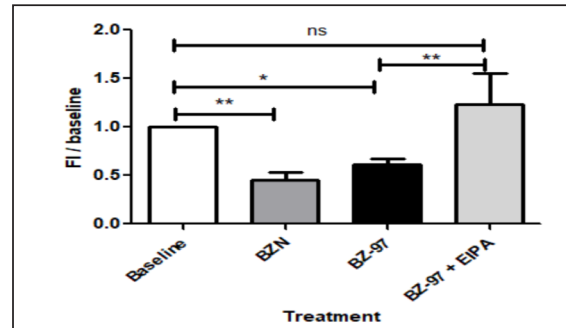

Figure 8. FM image processing analysis.

Epimastigotes of *T. cruzi* strain Y were treated with LIT medium (control), 20 µM BZ-97, 20 µM BZ-97 + 5 µM EIPA or 40 µM BNZ for 24 h and were assayed using the LysoSensor Green probe. FM Image processing and analysis was performed using ImageJ software. Each data is expressed as a FI over baseline (control, LIT medium- treated epimastigote). One-way ANOVA and Bonferroni's Multiple Comparison Test were used. *** $p < 0.001$; ns: no significant difference.

Intracellular calcium mobilization induced by BZ-97

This study investigated the initial response (first few minutes) of *T. cruzi* epimastigotes to BZ-97, and compared it to the reference drug BNZ. The release of calcium ions into the cytoplasm, a key signaling event, was monitored using the calcium-binding dye Cal-520 for a period of 2.5 h (Figure 9).
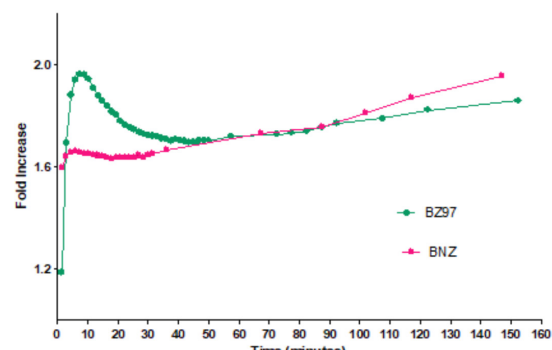

Figure 9. Cytosolic Calcium Changes.

BZ-97: a promising compound against Trypanosoma cruzi

T. cruzi epimastigotes were incubated with either 20 µM BZ-97 or 40 µM BNZ. Acridine Orange (5 µM) was subsequently added before fluorescence measurements were taken every 60 seconds for the initial 50 minutes following treatment. Thereafter, readings were collected at less frequent intervals. The data presented represent fold-changes relative to the baseline.

Both BZ-97 and BNZ induce a rapid rise in cytoplasmic calcium levels in *T. cruzi* epimastigotes. While BZ-97 exhibits a faster initial increase compared to BNZ, this effect appears transient. Following the initial peak, the calcium levels induced by BZ-97 progressively decrease, reaching a similar level of that observed with BNZ for over the next 30 minutes. In parasites treated with BNZ, however, the levels of mobilized calcium continue augmenting until it is almost double that of control parasites at the final measured time point.

Effect of early BZ-97 exposure on epimastigotes apoptosis induction.

Given that a significant effect on acidocalcisomes acidity is detected as soon as 3 h of BZ-97 treatment, we evaluated the effect of this compound on the induction of apoptosis at this time point. Apoptotic cells can be distinguished from necrotic cells using propidium iodide (PI), as PI can enter necrotic cells with damaged membranes.

Viable epimastigotes were treated with 20 µM BZ-97 or 40 µM BNZ for 3 h prior to PI staining, and changes in their fluorescence were assessed using flow cytometry. Figure 10 shows no significant differences between untreated and treated epimastigotes, indicating no signs of apoptosis as early as 3 hours after exposure to these compounds. Heating the parasites to 80oC, a very aggressive treatment for the membranes, shows a high fluorescence increment (incorporation of PI).
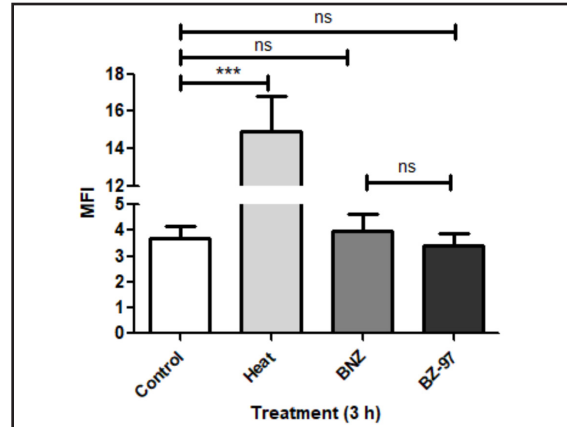

Figure 10. Effect of early BZ-97 exposure on epimastigote apoptosis.

Epimastigotes of the Y strain of *T. cruzi* were treated with 20 µM BZ-97, 40 µM BNZ for 3 h, or submitted to heating at 80 °C for 30 min. PI was added to all groups, and their fluorescence was analyzed using flow cytometry. MFI: Mean Fluorescence Intensity. One-way ANOVA and Bonferroni's Multiple Comparison Test were used. ns: not significant.

Effect of long-lasting exposure to BZ-97 on the induction of epimastigote apoptosis

In order to assess whether BZ-97 treatment for 6 and 24 h induces changes in epimastigote viability through apoptosis or necrosis, additional experiments were conducted using the Alexa Fluor® 488 Annexin V/Dead Cell Apoptosis assay. Cells were classified according to these conditions: Annexin V+/PI- (early apoptotic cells), Annexin V+/PI+ (Late apoptotic/ necrotic cells), Annexin V-/PI- (Viable cells) and Annexin V-/PI+ (necrotic cells).

Viable epimastigotes were treated with 20 µM BZ-97, 40 µM BNZ or 1 µM staurosporine for 6 and 24 h and changes in PI uptake and Annexin V cell-associated fluorescence were assessed using flow cytometry.

Data obtained at 6 hours post-incubation indicates that staurosporine induces a mild but significant shift towards Annexin V-/PI+ epi-

mastigotes (necrotic cells) as follows: untreated (0.12% ± 0.02%), staurosporine (4.16% ± 0.08%), BNZ (0.11% ± 0.05%), and BZ-97 (0.17% ± 0.05%). Thus, staurosporine vs BZ-97-treated, BNZ-treated, or untreated parasites show significance (p < 0.001). BZ-97-treated, BNZ-treated, and untreated epimastigotes do not differ significantly from each other (ANOVA and Bonferroni's Multiple Comparison Test). Figure 11 shows a representative 2D dot plot of FL1 (Annexin V) vs FL2 (PI) obtained from the flow cytometry analysis of epimastigotes subjected to treatment.
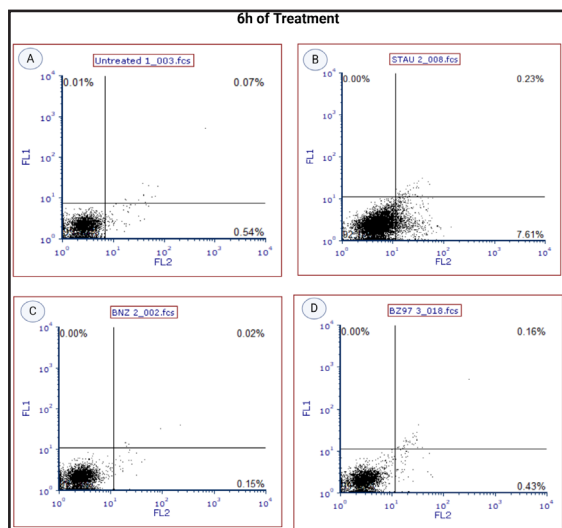

Figure 11. Changes in Fluorescence intensity on epimastigote population following 6 h of staurosporine, BNZ or BZ-97 treatment.

Representative 2D scatter plots (FL1 vs FL2) obtained from flow cytometry analysis of *T. cruzi* epimastigotes strain Y treated for 6 h with culture medium (A), 1 µM staurosporine (B), 40 µM BNZ (C) or 20 µM BZ-97 (D). Values in each quadrant represent the percentage (%) of parasites analyzed which fall on each one of them.

Data obtained at 24 hours post-incubation show significant differences in Annexin V-/PI+ epimastigotes (necrotic cells) as follows: untreated (3.15% ± 1.51 %), staurosporine (50.36 ± 8.8 %), BNZ (2.793 ± 1.03 %), and BZ-

97 (11.43 ± 2.18 %). The difference between staurosporine and untreated cells is highly significant (p < 0.001), whereas no significant differences were observed between BZ-97-treated, BNZ-treated or untreated cells (ANOVA and Bonferroni's Multiple Comparison Test). See Figure 11 for a representative sample.

Annexin V+/PI+ epimastigotes (late apoptotic/necrotic cells) also show differences as follow: untreated (1.08% ± 0.66 %), staurosporine (11.48 ± 3.9 %), BNZ (4.17 ± 1.59 %), and BZ-97 (8.51 ± 0.8 %). For the comparison between staurosporine vs untreated parasites, the difference between staurosporine and the untreated trypanosomatids is highly significant (p< 0.001), whereas no significant differences were observed between BZ-97-treated, BNZ-treated or untreated cells. staurosporine vs BZ-97 or BNZ did not show significant differences suggesting that both imidazoles exert a mild but significant pro-apoptotic effect (ANOVA and Bonferroni's Multiple Comparison Test).

Figure 12 shows a representative 2D dot plot of FL1 (Annexin V) vs FL2 (PI) obtained from the flow cytometry analysis of epimastigotes treated for 24 h.
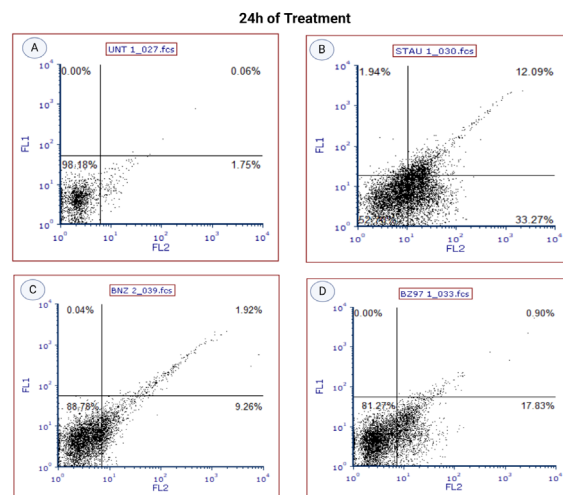

Figure 12. Changes in Fluorescence intensity on epimastigote population following 6h of staurosporine, BNZ or BZ-97 treatment.

Representative 2D scatter plots (FL1 vs. FL2) obtained from flow cytometry analysis of *T. cruzi epimastigotes* treated with culture medium (A), 1 µM staurosporine (B), 40 µM BNZ (C), or 20 µM BZ-97 (D) for 24 h. Values in each quadrant represent the percentage (%) of parasites, from the total acquired, in each one of the quadrants.

Effect of treatments on epimastigote structure and morphology

Figure 13 depicts the results of flow cytometry analysis, where epimastigotes exposed to various treatments are represented as a dot plot based on their fluorescence intensity in two channels (FL1: Annexin V, FL2: PI). Quadrant Q2 encompasses parasites positive for both Annexin V and PI (Annexin V+/PI+). Notably, staurosporine and BZ-97 treatment resulted in the highest proportion of cells in Q2, suggesting a promotion of apoptosis.

We also assessed the impact of these compounds on parasite cellular complexity using flow cytometry, with FSC (forward scatter) and SSC (side scatter) serving as measures of cell size and granularity, respectively.

After 6 h of treatment, epimastigotes treated with staurosporine exhibited significant changes in parasite complexity. This was indicated by the appearance of a new cellu-

lar sub-population in the lower left quadrant, demonstrating notable differences in both size (FSC, forward scatter) and granularity (SSC, side scattering) compared to the control. Experimental epimastigotes create a new population as follows: untreated (6.37 % ± 0.42 %), staurosporine- (29.87 ± 0.89 %), BNZ- (6.17 ± 0.14 %), and BZ-97- treated (7.65 ± 0.67 %). The difference between staurosporine and BZ-97-treated and BNZ-treated or untreated cells is highly significant ($p<0.001$), whereas no significant differences were observed between BZ-97-treated, BNZ-treated or untreated cells. (ANOVA and Bonferroni's Multiple Comparison Test).

After 24 h of treatment, the percentage of cells in the lower left quadrant increased dramatically in all groups, to finish as follows: untreated (31.7 ± 4.85 %), staurosporine (64.7 ± 0.81%), BNZ (62.17 ± 10.2%), and BZ-97 (64.38 ± 0.63%). The difference between untreated epimastigotes vs those treated with staurosporine, BZ-97 or BNZ is highly significant ($p<0.001$). No significant differences between treated cells were observed (ANOVA and Bonferroni's Multiple Comparison Test).

Figure 12 shows representative 2D scatter dot plots (FSC vs SSC) reflecting epimastigote complexity after being subjected to treatment for 6 h and 24 h.
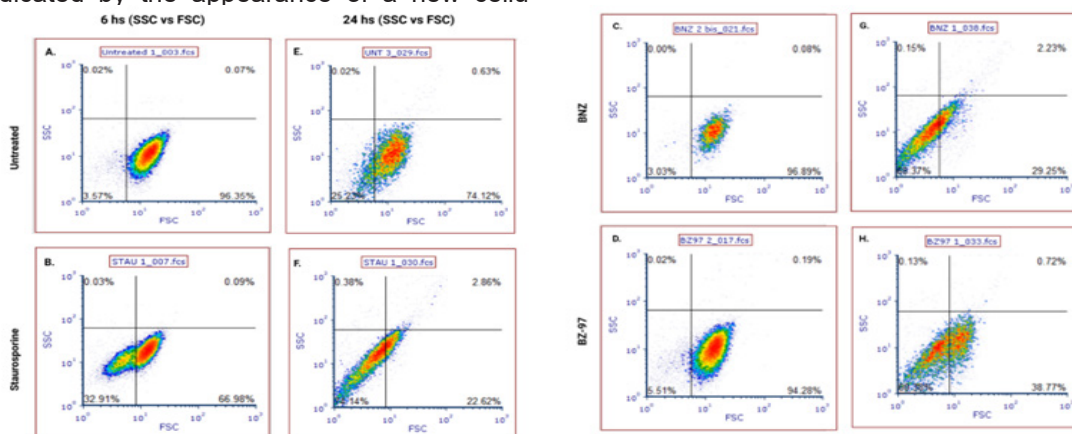

Figure 13. Changes in the complexity of the epimastigote population following BZ-97, BNZ, or staurosporine treatment for 6 and 24 h.

Botacio *et al*

Representative 2D scatter dot plots (FSC vs SSC) reflecting epimastigote complexity were obtained by flow cytometry data analysis. Dot plots from *T. cruzi* epimastigotes treated with culture medium, 1 µM staurosporine, 40 µM BNZ, or 20 µM BZ-97 for 6 h (Figures A, B, C, and D, respectively) and for 24 h (Figures E, F, G, and H, respectively) were divided into four quadrants (Q1-Q4). Q1 and Q2 represent the upper left and right quadrants, respectively, while Q3 and Q4 represent the lower left and right quadrants, respectively. This division was performed to evaluate the percentage of cells in each quadrant (A-F).

Given the observed changes in the morphological complexity of epimastigotes in the SSC vs FSC Lower Left Quadrant after 24 h of treatment, we proceeded to evaluate cell death parameters. After establishing the role of acidocalcisomes in BZ-97 treatment, we study the type of death the parasites were being driven with its treatment, in this specific population.

The results are depicted in Figure 14 and show that the treated epimastigote population predominantly consisted of viable cells (Annexin V-/PI-) except when exposed to staurosporine, which significantly reduced cell viability.

Staurosporine treatment also led to a notable increase in the percentage of necrotic cells (Annexin V-/PI+), whereas BZ-97 or BNZ did not markedly affect this form of cell death. Regarding the late apoptotic/necrotic cell population, approximately 10% of staurosporine-treated epimastigotes underwent this type of cell death. BZ-97 exhibited a mild effect, showing no significant differences from BNZ. Additionally, while the percentage of early apoptotic cells was generally low, it was higher in the group treated with BZ-97 compared to the other treatments.
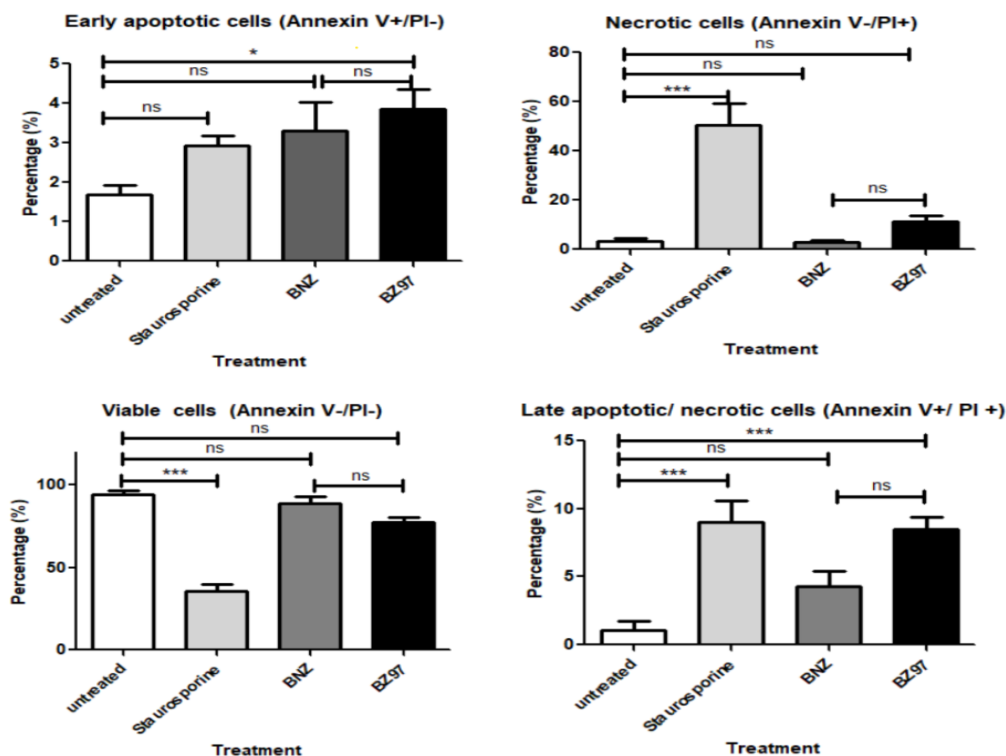

Figure 14. Morphology changes after drug treatment.

BZ-97: a promising compound against Trypanosoma cruzi

Epimastigotes were treated with 1 µM staurosporine, 40 µM BNZ or 20 µM BZ-97. After 24 h of incubation they were stained with Annexin V and Propidium Iodide and analyzed by flow cytometry with the use of quadrants: Annexin V+/PI− (early apoptotic parasites): V+/PI+ (late apoptotic or necrotic parasites);: Annexin V−/PI− (viable parasites); Annexin V-/PI+ (necrotic parasites). * p< 0.05, *** p< 0.001. One-way ANOVA and Bonferroni's Multiple Comparison Test were used. ns: not significant.

Discussion

Chagas disease (CD), caused by the hemoflagellate *Trypanosoma cruzi* parasite, is a neglected tropical disease endemic to the Americas, affecting over six million individuals (21) (CDC, 2022). While originally confined to this region, migration and environmental changes have propelled CD to a global public health concern (22).

Despite continuous exploration of new treatment possibilities (23), only nitrofurans like nifurtimox (NFX) and the 2-nitroimidazole derivative benznidazole (BNZ), discovered in the early 1960s, remain the mainstay of therapy (22).

Following a 2010 stakeholders' summit in Rio de Janeiro, Brazil, researchers established criteria for further evaluation of Chagas disease drug candidates. These criteria included having an IC50 (concentration inhibiting 50% of parasite growth) equal to or lower than BNZ and a selectivity index (ratio of cytotoxicity to antiparasitic activity) above 10 (16). The benzimidazole derivative BZ-97 fulfilled both criteria in the antiparasitic intracellular assays, warranting further investigations into the compound's mechanism of action against *T. cruzi*.

Given the well-documented association between various drug treatments and the induction of reactive oxygen species (ROS) synthesis as a result of oxidative stress, we first examined the effects of BZ-97 on ROS generation within its target. In fact, ROS production is a marker of alterations in the parasite's homeostasis, i.e., anti- *T. cruzi* treatments (24), hypoxia (25), heme presence as a consequence of heme release during blood digestion (26, 27), starvation and pH stress (28). Elevated ROS production triggers metabolic adaptations in *T. cruzi.* For instance, hypoxia reduces mitochondrial function and energy production, leading to a further increase in ROS (29). Reactive species, thus, can act as a double-edged sword. Studies have demonstrated its diverse effects on the parasite: triggering self-cleaning (autophagy), programmed cell death (apoptosis), or even proliferation (28). Interestingly, when ROS signals proliferation, the parasite's ability to transform into its infective form (metacyclogenesis) is simultaneously suppressed (25).

Our findings indicate that, unlike BNZ, treatment with BZ-97 for 3 hours does not significantly alter the levels of ROS or the mitochondrial membrane potential in *T. cruzi* epimastigotes. This suggests that BZ-97 does not substantially disrupt the mitochondrial electron transport chain, a known source of ROS generation. In contrast, BNZ treatment rapidly induces a significant increase in ROS production and alters the mitochondrial membrane potential within 3 hours. These observations suggest distinct mechanisms of action for these structurally similar imidazole derivatives.

Acidocalcisomes are small, mostly spherical, acidic organelles with an average diameter ranging from 0.2 to 0.6 µm (30). These organelles have several functions including cation and phosphorus storage (31), autophagy, osmoregulation (32), pH homeostasis, and pathogenesis (33). Recent studies have established the role of these organelles not only in phosphate utilization and calcium ion signaling but also on bioenergetics (32) (Docampo et al, 2022). In fact, being the main intracellular reservoir of calcium and phosphate, acidocalcisomes can contribute to signaling in specific processes like pH, homeostasis, and other metabolic processes (32,34,35). It is well known that Ca^{2+}

in the acidocalcisome is bound to a polyanionic matrix of poly P, and can be released after alkalinization of the organelle. This pivotal role underscores their importance in cellular function.

Our data indicate that BZ-97 is able to induce acidocalcisome alkalinization in a similar way as BNZ, which was previously reported as deprotonating the organelle (36). As a control in our experiments, epimastigotes were also subjected to hyperosmotic stress induced by 5 µM Mannitol, leading to alkalinization of acidic vacuoles via a Na+/H+ exchanger (NHE). The BZ-97 and BNZ effects were both blocked by 5-(N-ethyl-N-isopropyl)amiloride (EIPA), an NHE inhibitor, demonstrating the involvement of this pump in the effects caused by the imidazole derivatives.

Differently, the effect of Mannitol was only partially reversed by EIPA. It is important to note that these latter results are not in agreement with those reported by Usorach et al, 2021 (37).

After establishing the role of acidocalcisomes in BZ-97 treatment, we investigated the type of death the parasites were being driven with its treatment. Thus, we used the combination of Annexin V binding and PI uptake, as it is one of the most commonly used assays to measure apoptosis (38). The technique uses double staining with Annexin V, which binds to phosphatidylserine when exposed to the outside of the cytoplasmic membrane as a sign of apoptosis, and PI, since this dye can enter necrotic cells but not early apoptotic cells.

Epimastigotes were analyzed for PI uptake and Annexin V cell-associated fluorescence by flow cytometry at 6 and 24 h. Staurosporine, a protein kinase inhibitor often used to induce apoptosis, was used as a positive control for this process. The use of quadrants helped divide the parasites studied into four possible combinations: Annexin V+/PI- (early apoptotic), Annexin V+/PI+ (late apoptotic), Annexin V-/PI- (viable), Annexin V-/PI+ (necrotic).

Data obtained at 6 hours post-incubation with all drugs indicates that only staurosporine induces a mild but significant shift towards Annexin V-/PI+ epimastigotes indicating that some necrosis is taking place, only with that treatment.

When analyzing the results of the Annexin V+/PI+ epimastigotes (late apoptotic/ necrotic cells) at t= 6 h, BNZ-treated parasites show very little apoptosis induction. As for BZ-97, even though the difference is not significant, it already seems to induce more apoptosis than BNZ, once again suggesting a different route of action for both molecules when acting on *T. cruzi* epimastigotes.

Staurosporine, used as a positive control, demonstrated the highest percentage of Annexin V+/PI+ cells, highlighting its significant pro-apoptotic effect. Both BZ-97 and BNZ also increased the proportion of Annexin V+/PI+ but to a lesser extent, compared to the untreated control. Furthermore, no significant differences were observed between BZ-97 and BNZ treatments, indicating that both imidazoles induce a moderate but comparable increase in late-stage apoptosis. It is worth considering several factors that must be taken into account when monitoring the detection of apoptotic markers: (i) Parasite life cycle: *T. cruzi* cell cycle extends beyond 24 hours. The peak apoptotic response induced by BZ-97 and BNZ might occur after this timeframe. (ii) Atypical PS translocation: Imidazoles like BZ-97 and BNZ could potentially trigger alternative apoptotic pathways that do not involve substantial phosphatidylserine (PS) exposure on the cell surface. (iii) Limitations of the assay: As demonstrated by Menna-Barreto et al. (2009), Annexin V/PI staining might not always be sensitive enough to detect apoptosis in T. cruzi epimastigotes, even when other apoptotic markers are present.

The lack of a strong phosphatidylserine (PS) signal in this study does not necessarily exclude apoptosis as a cell death mechanism. In this context, the more detailed information

provided by flow cytometry analysis is worth analyzing, as described below.

Flow cytometry analysis was done to analyze the parasite cellular complexity using epimastigotes exposed to various treatments which were represented as dot plots where FSC (forward scatter) and SSC (side scatter) served as measures of cell size and granularity, respectively. After 6 h of treatment, epimastigotes treated with staurosporine showed significant changes in parasite complexity. This was evidenced by the emergence of a new cellular subpopulation in the lower-left quadrant, characterized by noticeable differences in both size (FSC, forward scatter) and granularity (SSC, side scattering) compared to the control. Experimental epimastigotes fell into a new population where the staurosporine-treated epimastigotes formed the majority of them, with a minor and almost equal representation from the other three groups. The difference between staurosporine and BZ-97-treated, BNZ-treated, and untreated cells is highly significant (p<0.001), whereas no significant differences were observed between the latter three groups. By t=24 h, however, the shift to the lower left quadrant is notorious. This suggests that the treatments' effects have impacted the morphology of the parasites, making them smaller and/or less complex.

Further analysis of the cells in this quadrant using FL1 (Annexin V) and FL2 (PI) revealed that approximately 80% of the BZ-97- or BNZ-treated population exhibited morphological changes while remaining viable. This suggests that these drugs primarily induce structural alterations without immediately causing cell death. The precise mechanism underlying these morphological changes in BZ-97-treated cells remains unclear and cannot be definitively determined based solely on the current experiments presented here. While microscopic observations also revealed altered parasite shapes, further investigation is required to elucidate the specific pathways involved.

In addition, the increase of untreated epimastigotes in Q3 indicates that around 30% of the epimastigotes die as a result of an effect not attributable to these compounds.

Our findings suggest that while BZ-97 shares various mechanisms of action with BNZ, it likely targets distinct cellular processes, leading to divergent effects. This is supported by the lack of significant ROS production and the minimal disruption of mitochondrial function observed upon BZ-97 treatment, as discussed below.

Only BNZ appears to alter mitochondrial oxidative phosphorylation, as evidenced by the increased production of reactive oxygen species observed in parasites stimulated by this compound. On the other hand, both BZ-97 and BNZ induce a clear effect on the alkalinization of acidocalcisomes. This is confirmed by studies using acridine orange and LysoSensor, the latter being a probe capable of interacting with the parasite's acidic compartments.

BZ-97 would deliver a pro-apoptotic effect, rather than a necrotic one, on epimastigotes subjected to its treatment. This effect becomes evident after 24 hours of treatment, providing an indication of when the treatment's effect becomes apparent, despite indications that BZ-97, like BNZ, begins to exert effects on the parasite's physiology in the early stages (3 or 6 h) of treatment. This observation is a relevant issue for it would mean that this compound is capable of causing death on the parasite without giving rise to inflammatory processes that result from necrosis.

It is worth noting that in microscopy studies, epimastigotes treated with BZ-97 experienced morphological changes, appearing more "stout" with rounder, less elongated bodies (data not shown). This morphological change is reflected in flow cytometry studies on cellular complexity. There, it is observed that at 24 hours, cellular subpopulations of smaller size and lower granularity appear. These changes are not necessarily accompanied by a decrease

in cell viability, as Annexin V/PI studies on these cells indicate that the majority of cells are viable, with only a small percentage undergoing early apoptosis (around 4%) and even fewer undergoing late apoptosis/necrosis (less than 10%). Similar results are observed with BNZ, with both being significantly different from those obtained from epimastigotes treated with staurosporine.

It is worth noticing that all the effects observed with BZ-97 occur at a dose twice as low as that of BNZ. The fact that this compound can exert a similar effect to one of the treatments considered the gold standard to tackle Chagas Disease deserves further investigation and consideration as a potential therapeutic option for the future.

DECLARATIONS

Acknowledgments

Ethical approval
Not Applicable

Funding

Availability of data and materials

All data and materials presented here are offered upon request but are subject to availability

Competing Interests

All authors declare not to have any financial or non-financial interest in this publication.

Author Contributions

Conceptualization, RC, CS; Methodology, MB, MFER, MN, LMN, JC, RC; Validation, MFER, JC, EdO, CS; Formal analysis, MB, MFER, MN, RC, CS; Investigation, MB, MFER, NE, MN, LMN, JC, DD, LP, RC, CS; Resources, EdO, CS; Data curation, JC, CS; Writing – original draft, MFER; Writing – review & editing, MB, MFER, NE, MN, LMN, JC, DD, LP, EdO, RC, CS; Visualization, MFER; Supervision, MFER, MN, LMN, LP, EdO, CS; Project administration, CS.

All authors read the final manuscript and approved it.

References

1. CDC website. https://www.cdc.gov/parasites/chagas/epi.html (Accessed on March, 2024)

2. WHO, 2022. World Chagas Disease Day: finding and reporting every case (who.int) (Accessed March 4, 2024)

3. Echeverría L. E., Marcus R., Novick, G., Sosa-Estani S., Ralston K., Zaidel E. J., Forsyth C., Ribeirobn A. L. P., Mendoza I., Falconi M. L., Mitelman J., Morillo C. A., Pereiro A. C., PinazonmM. J., Salvatella R., Martinez F., Perel P., Liprandi Á. S., Piñeiro D. J., & Molina, G. R. *WHF IASC Roadmap on Chagas Disease. Glob Heart.* 2020; 30; 15(1):26. doi: 10.5334/gh.484. PMID: 32489799; PMCID: PMC7218776.

4. Pinheiro E., Brum-Soares L., Reis R., & Cubides J. C. (2017). Chagas disease: review of needs, neglect, and obstacles to treatment access in Latin America. *Revista Da Sociedade Brasileira de Medicina Tropical* 2016; 50: 296–300. https://doi.org/10.1590/0037-8682-0433-2016.

5. Monge-Maillo B., López-Vélez R. Challenges in the management of Chagas disease in Latin-American migrants in Europe. *Clin Microbiol Infect.* 2017; 23 :290-295. doi: 10.1016/j.cmi.2017.04.013.

6. Prata A. Clinical and epidemiological aspects of Chagas disease. *Lancet Infect Dis*. 2001; 1:92-100. doi: 10.1016/S1473-3099(01)00065-2.

7. Meymandi S., Hernandez S., Park S., Sanchez DR., Forsyth C. Treatment of Chagas Disease in the United States. *Curr Treat Options Infect Dis*. 2018; 10:373-388. doi: 10.1007/s40506-018-0170-z. Epub 2018 Jun 26. PMID: 30220883; PMCID: PMC6132494.

8. Castro J.A, de Mecca M.M., Bartel L.C. Toxic side effects of drugs used to treat Chagas' disease (American trypanosomiasis). *H*µM *Exp Toxicol*. 2006 Aµg;25(8):471-9. doi: 10.1191/0960327106het653oa.

9. Rassi A., Rassi A., Marcondes de Rezende J.. American Trypanosomiasis (Chagas Disease). *Infect Dis Clin North Am*. 2012;26:275–291. doi: 10.1016/j.idc.2012.03.002.

10. Pérez-Molina J.A, Molina I. Chagas disease. The Lancet. 2018;391(10115):82–94. doi: 10.1016/S0140-6736(17)31612-411. Castro J.A., de Mecca M.M., Bartel L.C. Toxic side effects of drugs used to treat Chagas' disease (American trypanosomiasis). *Hum Exp Toxicol*. 2006; 25:471-9. doi: 10.1191/0960327106het653oa.

11. Turrens J.F., Watts B.P. Jr, Zhong L., Docampo R. Inhibition of Trypanosoma cruzi and T. brucei NADH fumarate reductase by benznidazole and anthelmintic imidazole derivatives. *Mol Biochem Parasitol*. 1996; 82: 125-9. doi: 10.1016/0166-6851(96)02722-3. PMID: 8943158.

12. Edwards D.I. Nitroimidazole drugs--action and resistance mechanisms. I. Mechanisms of action. *J Antimicrob Chemother*. 1993; 31:9-20. doi: 10.1093/jac/31.1.9. PMID: 8444678.

13. Escala E., Valderas-García E., Álvarez Bardón M., Castilla Gómez de Agüero V., López-Pérez J.L., Rojo-Vázquez F.A., San Feliciano A., Martínez-Valladares M., Balaña-Fouce R., del Olmo E. Further and new target-based benzimidazole anthelmintics active against *Teladorsagia circumcincta. Journal of Molecular structure* 2022; 1269: 133735 doi.org/10.1016/j.molstruc.2022.133735

14. Buckner F.S., Verlinde C.L., La Flamme A.C., Van Voorhis W.C. Efficient technique for screening drugs for activity against Trypanosoma cruzi using parasites expressing beta-galactosidase. *Antimicrob Agents Chemother*. 1996; 40: 2592-7. doi: 10.1128/AAC.40.11.2592. PMID: 8913471; PMCID: PMC163582.

15. Romanha A.J., Castro S.L., Soeiro M de N., Lannes-Vieira J., Ribeiro I., Talvani A., Bourdin B., Blum B., Olivieri B., Zani C., Spadafora C., Chiari E., Chatelain E., Chaves G., Calzada J.E., Bustamante J.M., Freitas-Junior L.H., Romero L.I., Bahia M.T., Lotrowska M., Soares M., Andrade S.G., Armstrong T., Degrave W., Andrade Z de A. In vitro and in vivo experimental models for drug screening and development for Chagas disease. *Mem Inst Oswaldo Cruz*. 2010; 105:233-8. doi: 10.1590/s0074-02762010000200022.

16. Mosmann T. Rapid colorimetric assay for cellular growth and survival: application to proliferation and cytotoxicity assays. *J Immunol Methods*. 1983; 65: 55-63. doi: 10.1016/0022-1759(83)90303-4.

17. Muelas-Serrano S., Nogal-Ruiz J.J., Gómez-Barrio A. Setting of a colorimetric method to determine the viability of Trypanosoma cruzi epimastigotes. *Parasitol Res*. 2000; 86:999-1002. doi: 10.1007/pl00008532.

18. Sabnis R.W., Deligeorgiev T.G., Jachak M.N., Dalvi T.S. DiOC6(3): a useful dye for staining the endoplasmic reticulum. *Biotech Histochem*. 1997; 72: 253-8. doi: 10.3109/10520299709082249. PMID: 9408585.

19. Palmgren M.G. Acridine orange as a probe for measuring pH gradients across membranes: mechanism and limitations. *Anal Biochem*. 1991; 192: 316-21. doi: 10.1016/0003-2697(91)90542-2.

20. Albrecht L.V., Tejeda-Muñoz N., De Robertis E.M. Protocol for Probing Regulated Lysosomal Activity and Function in Living Cells. *STAR Protoc*. 2020; 1: 100132. doi: 10.1016/j.xpro.2020.100132.

21. CDC. Updated Estimates and Mapping for Prevalence of Chagas Disease among Adults, United States - *Emerging Infectious Diseases journal* 2022; 28: 7.

22. Gómez-Ochoa S.A., Rojas L.Z., Echeverría L.E., Muka T., Franco O.H. Global, Regional, and National Trends of Chagas Disease from 1990 to 2019: Comprehensive Analysis of the Global Burden of Disease Study. *Glob Heart*. 2022; 17: 59. doi: 10.5334/gh.1150

23. Mazzeti A.L., Capelari-Oliveira P., Bahia M.T., Mosqueira V.C.F. Review on Experimental Treatment Strategies Against *Trypanosoma cruzi*. *J Exp Pharmacol*. 2021; 13: 409-432. doi: 10.2147/JEP.S267378.

24. Bombaça A.C.S., Viana P.G., Santos A.C.C., Silva T.L., Rodrigues A.B.M., Guimarães A.C.R., Goulart M.O.F., da Silva Júnior E.N., Menna-Barreto R.F.S. Mitochondrial disfunction and ROS production are essential for anti-*Trypanosoma cruzi* activity of β-lapachone-derived naphthoimidazoles. *Free Radic Biol Med*. 2019; 130: 408-418. doi: 10.1016/j.freeradbiomed.2018.11.012.

25. Saraiva F.M.S., Cosentino-Gomes D., Inacio J.D.F., Almeida-Amaral E.E., Louzada-Neto O., Rossini A., Nogueira N.P., Meyer-Fernandes J.R., Paes M.C. Hypoxia Effects on *Trypanosoma cruzi* Epimastigotes Proliferation, Differentiation, and Energy Metabolism. *Pathogens*. 2022; 11: 897. doi: 10.3390/pathogens11080897.

26. Nogueira N.P., de Souza C.F., Saraiva F.M., Sultano P.E., Dalmau S.R., Bruno R.E., Gonçalves Rde.L., Laranja G.A., Leal L.H., Coelho M.G., Masuda C.A., Oliveira M.F., Paes M.C.. Heme-induced ROS in Trypanosoma cruzi activates CaMKII-like that triggers epimastigote proliferation. One helpful effect of ROS. *PLoS One*. 2011; 6: e25935. doi: 10.1371/journal.pone.0025935.

27. Nogueira N.P., Saraiva F.M.S., Oliveira M.P., Mendonça A.P.M., Inacio J.D.F., Almeida-Amaral E.E., Menna-Barreto R.F., Laranja G.A.T., Torres E.J.L., Oliveira M.F., Paes M.C. Heme modulates *Trypanosoma cruzi* bioenergetics inducing mitochondrial ROS production. *Free Radic Biol Med*. 2017; 108: 183-191. doi: 10.1016/j.freeradbiomed.2017.03.027.

28. Pedra-Rezende Y., Fernandes M.C., Mesquita-Rodrigues C., Stiebler R., Bombaça A.C.S., Pinho N., Cuervo P., De Castro S.L., Menna-Barreto R.F.S. Starvation and pH stress conditions induced mitochondrial dysfunction, ROS production and autophagy in Trypanosoma cruzi epimastigotes. *Biochim Biophys Acta Mol Basis Dis*. 2021; 1867: 166028. doi: 10.1016/j.bbadis.2020.166028.

29. Kung-Chun C.D., Pui-Wah T.A., Law C.T., Ming-Jing X.I., Lee D., Chen M., Kit-Ho L.R, Wai-Hin Yuen V, Wing-Sum Cheu J, Wai-Hung Ho D, Wong CM, Zhang H, Oi-Lin

Ng I, Chak-Lui Wong C. Hypoxia regulates the mitochondrial activity of hepatocellular carcinoma cells through HIF/HEY1/PINK1 pathway. *Cell Death Dis*. 2019; 10: 934. doi: 10.1038/s41419-019-2155-3.

30. Docampo R., de Souza W., Miranda K.*, Rohloff P., Moreno S.N.J*. Acidocalcisomes? conserved from bacteria to man. *Nat Rev Microbiol* 2005; 3; 251. https://doi.org/10.1038/nrmicro1097

31. Docampo R., Moreno S.N. Acidocalcisomes. *Cell Calcium*. 2011; 50: 113. doi: 10.1016/j.ceca.2011.05.012.

32. Docampo R., Huang G. New insights into the role of acidocalcisomes in trypanosomatids. *J Eukaryot Microbiol*. 2022; 69:e12899. doi: 10.1111/jeu.12899.

33. Li F.J., He C.Y. Acidocalcisome is required for autophagy in Trypanosoma brucei. *Autophagy*. 2014;10(11):1978-88. doi: 10.4161/auto.36183.

34. Benaim G., Paniz-Mondolfi A.E., Sordillo E.M., Martinez-Sotillo N. Disruption of Intracellular Calcium Homeostasis as a Therapeutic Target Against *Trypanosoma cruzi*. Front *Cell Infect Microbiol*. 2020;10: 46. doi: 10.3389/fcimb.2020.00046

35. Serrano-Martín X., García-Marchan Y., Fernandez A., Rodriguez N., Rojas H., Visbal G., Benaim G. Amiodarone destabilizes intracellular Ca2+ homeostasis and biosynthesis of sterols in Leishmania mexicana. *Antimicrob Agents Chemother*. 2009 Apr;53(4):1403-10. doi: 10.1128/AAC.01215-08. Epub 2009 Jan 21. PMID: 19164149; PMCID: PMC2663059.

36. Mantilla B.S., Azevedo C., Denny P.W., Saiardi A., Docampo R. The Histidine Ammonia Lyase of *Trypanosoma cruzi* Is Involved in Acidocalcisome Alkalinization and Is Essential for Survival under Starvation Conditions. *mBio*. 2021; 12: e0198121. doi:10.1128/mBio.01981-21.

37. Usorach M., Gimenez A.M., Peppino Margutti M., Racagni GE., Machado E.E. Calcium Signaling Involves Na^+/H^+ Exchanger and IP_3 Receptor Activation in *T. cruzi* Epimastigotes. *Biologics*. 2021 :384-395. https://doi.org/10.3390/biologics1030022.

38. Reutelingsperger C.P., van Heerde W.L. Annexin V, the regulator of phosphatidylserine-catalyzed inflammation and coagulation during apoptosis. *Cell Mol Life Sci*. 1997; 53:527-32. doi: 10.1007/s000180050067.

39. Menna-Barreto RF., Corrêa J.R., Cascabulho C.M., Fernandes M.C. Pinto A.V. Soares M.J., De Castro S.L. Naphthoimidazoles promote different death phenotypes in Trypanosoma cruzi. *Parasitology*. 2009 ;136 :499-510. doi: 10.1017/S0031182009005745.